Title:

Dissecting the interaction between transglutaminase 2 and fibronectin

Authors

Inês Cardoso[1], Eva Christina Østerlund[2], Jorunn Stamnaes[1], Rasmus Iversen[1], Jan Terje Andersen[1, 3], Thomas J. D. Jørgensen[2], Ludvig M. Sollid[1]

Author affiliations

[1] Centre for Immune Regulation and Department of Immunology, University of Oslo and Oslo University Hospital, Oslo, Norway
[2] Department of Biochemistry and Molecular Biology, University of Southern Denmark, Odense M, Denmark
[3] Department of Biosciences, University of Oslo, Norway.

Corresponding author

Inês Cardoso
i.d.r.cardoso@medisin.uio.no
Telephone: +47 23074226
Fax: +47 23073510

Keywords

Transglutaminase 2

Fibronectin

Hydrogen/deuterium exchange

Site-directed mutagenesis

Surface plasmon resonance

Acknowledgements

This work was supported by the European Commission grants MRTN-CT-2006-036032 and ERC-2010-Ad-268541 and grants from the Research Council of Norway and the South-Eastern Norway Regional Health Authority. The authors thank Chaitan Khosla (Stanford University, CA; USA) for providing the TG3 plasmid.

Abbreviations

TG2, transglutaminase 2

FN, fibronectin

45FN, 45 kDa proteolytic fibronectin fragment (gelatin-binding domain)

ECM, extracellular matrix

HDX-MS, Hydrogen/deuterium exchange coupled with mass spectrometry

SPR, surface plasmon resonance

WT, wild-type

RH, TG2 mutant R116A/H134A

KRH, TG2 mutant K30E/R116A/H134A

mAb, monoclonal antibody

INTRODUCTION

Transglutaminase 2 (TG2) belongs to a family of calcium-dependent enzymes that catalyze cross-linking of proteins through formation of N-ε(γ-glutamyl)lysine isopeptide bonds between target glutamine and lysine residues (transamidation) (Mycek et al. 1959; Fuller and Doolittle 1966). The enzymatic activity of TG2 is implicated in biological processes such as wound healing (Stephens et al. 2004) and development of diseases like celiac disease (Sollid et al. 1997; Molberg et al. 1998). TG2 activity is subject to allosteric regulation through binding of effectors. Binding of Ca^{2+} is required for enzymatic activity (Clarke et al. 1959) whereas binding of GDP/GTP inhibits activity (Bergamini et al. 1987). Further, it is likely that protein-protein interactions may modulate the conformation and enzymatic activity of TG2. Binding of effectors can have dramatic effects on the structure of TG2, illustrated by crystallization of the enzyme in two distinct conformational states. In the structure of human TG2 with bound GDP or GTP, the enzyme adopts a "closed" conformation in which the two C-terminal domains are folded in and interact with the catalytic core domain (Liu et al. 2002; Jang et al. 2014). The structure of TG2 with a peptide inhibitor bound in the active site, on the other hand, reveals an "open" conformation in which the four globular domains are aligned to give an extended structure (Pinkas et al. 2007).

TG2 is expressed in the cytoplasm, but is also present in the extracellular environment, displayed at the cell surface or associated with the extracellular matrix (ECM) (Piacentini et al. 2014). The regulation and precise route of TG2 secretion from cells, however, remain debated (Zemskov et al. 2011; Adamczyk et al. 2015). The enzyme performs multiple functions depending on its localization, and TG2 can play several roles independently of its enzymatic activity (Lorand & Graham 2003; Zemskov et al. 2006). On the cell surface, TG2 acts as an integrin-binding co-receptor for fibronectin (FN), which promotes cell adhesion and migration (Akimov et al. 2000; Akimov & Belkin 2001), or associates with the heparan-sulfate chains of syndecan-4 (Scarpellini et al. 2009).

It is known that TG2 binds non-covalently to FN across species with high affinity (nM range) (Turner and Lorand 1989; LeMosy et al. 1992; Jeong et al. 1995; Achyuthan et al. 1996; Hang et al. 2005). FN is a glycosylated extracellular protein that exists as a 440 kDa homodimer linked by disulfide bonds (Mosesson et al. 1975). FN is abundantly present in plasma as a soluble protein, or it can be assembled into insoluble polymers as a critical part of the ECM

(Pankov 2002). The protein is essential for matrix assembly by serving as a scaffold for connection of several ECM components. Well-characterized FN domains, obtained as distinct fragments by proteolytic digestion, exhibit distinct binding properties and can interact with numerous ligands (Furie and Rifkin 1980; Ruoslahti et al. 1981). The 45 kDa domain in the N-terminal part of FN (45FN) (modules $I^{6}II^{1,2}I^{7-9}$), originally identified as the gelatin-binding domain (Engvall et al. 1978; Erat et al. 2009), is responsible for binding to TG2 (Radek et al. 1993). The 45FN domain retains the same binding affinity for TG2 as full-length FN (Radek et al. 1993). Furthermore, we recently demonstrated that FN is not the only interaction partner of TG2 in the ECM, as the FN-binding site of ECM-associated TG2 is exposed in tissue sections (Cardoso et al. 2015). However, given the high specificity and affinity of the interaction between TG2 and FN, it is likely that this interaction will dominate upon release of TG2 into the extracellular environment.

The FN-binding site of TG2 has previously been mapped to the N-terminal part of the enzyme (Jeong et al. 1995; Hang et al. 2005). The earliest study, performed with proteolytic fragments of purified guinea pig liver TG2, identified a sequence of seven amino acids (residues 2–8) as responsible for the binding to FN (Jeong et al. 1995). A more recent study, however, using recombinant human TG2 and several FactorXIIIa/TG2 chimeric proteins, defined residues D94 and D97 to be essential for binding to FN (Hang et al. 2005).

Given the lack of consensus in the literature and the importance of this interaction in TG2 biology, we here aimed to map and define the FN-binding site of human TG2. By combining different biochemical and biophysical methods, we confirm that the FN-binding site is located in the N-terminal domain of TG2 and that binding is not influenced by TG2 conformation. We identify evolutionarily conserved key residues that are crucial to mediate this high affinity interaction, and we show that FN binding likely also extends towards the catalytic core domain of TG2.

MATERIALS AND METHODS

Proteins

Recombinant human TG2 was obtained from Phadia as purified protein produced in Sf9 insect cells or expressed in *E. coli* as reported (Stamnaes et al. 2010) and purified by nickel-nitrilotriacetic acid affinity chromatography. TG2 mutants were produced in *E. coli* in the same way as wild-type (WT) human TG2. TG2 mutants and truncations were generated with the QuikChange Site-Directed Mutagenesis Kit (Stratagene) or by PCR amplification followed by subcloning of the fragments between the NdeI and HindIII restriction sites of the pET-28a vector (Novagen). The mutations were verified by DNA sequencing (GATC Biotech). Chimeric TG3/TG2 was obtained by PCR amplification of the N-terminal domain of TG3 (residues 1-136) and core and C-terminal domains of TG2 (residues 141-687), followed by assembly of the fragments by overlap extension PCR and subcloning into the pET-28a vector. High purity (>90%) of TG2 protein preparations was confirmed by SDS-PAGE, and absence of aggregates was verified by native PAGE. Correct conformational folding of all TG2 protein variants, except truncated TG2 1-143 was verified by assessing reactivity to conformational sensitive anti-TG2 monoclonal antibodies (mAbs). Most of the TG2 proteins were also tested for intact enzymatic activity levels by measuring deamidation of gliadin substrate peptide PQPQLPYPQPQLPY using matrix-assisted laser desorption ionization time-of-flight mass spectrometry as previously described (Stamnaes et al. 2008). In addition, protein stability was measured by differential scanning fluorimetry as described (Foss et al. 2016), using SYPO Orange (Sigma-Aldrich) at a 1:100 dilution, and a protein concentration of 0.1 mg/ml. Human 45FN was obtained from Sigma-Aldrich as a proteolytic fragment of human plasma FN.

Anti-TG2 antibodies

Human mAbs were produced as described previously (Di Niro et al. 2010). Briefly, expression vectors encoding the cloned antibody heavy and light chain V regions were co-transfected into HEK293F cells for expression of full-length IgG1 protein. mAbs were purified from cell supernatants by Protein G Sepharose (GE Healthcare), and the purity of the proteins was confirmed by SDS-PAGE. Biotinylation of the mAbs was done with EZ-Link® Sulfo-NHS-LC-Biotin (Thermo Scientific) according to the manufacturer's instructions, and excess free label was removed using Vivaspin ultrafiltration spin columns (Sartorius).

Effector-bound TG2

TG2 or TG2 1-465 was incubated with 2.5 mM of the TG2-inhibitor DP3-3 **(**Ac-P(DON)LPF-NH2 (DON = 6-diazo-5-oxo-L-norleucine, (Pinkas et al. 2007)) obtained from Zedira. This inhibitor reacts irreversibly with the active-site cysteine, thereby preventing self-cross-linking of TG2 in the presence of calcium, and maintains the enzyme in an open conformation (iTG2) (Pinkas et al. 2007). Incubation with the inhibitor for 15 min at room temperature was followed by addition of $CaCl_2$ to a final concentration of 10 mM. After 30 min incubation, excess free inhibitor was removed by use of a desalting column (Zeba spin column, Thermo Scientific), and the buffer was changed to TBS containing 5 mM $CaCl_2$ using a Vivaspin ultrafiltration spin column (Sartorius). For TG2 1-465, incubation with $CaCl_2$ and inhibitor was performed overnight, and excess inhibitor was removed by ion-exchange chromatography using a Mono Q HR column (GE Healthcare). To obtain TG2 in a closed conformation (GDP-TG2), the enzyme was incubated with 1 mM GDP for 1 h at room temperature.

Nondenaturing PAGE of TG2-FN complexes

Complexes between TG2 and FN were prepared by incubating equal molar amounts of WT iTG2, iTG2 1-465 or GDP-TG2 (prepared as described above) with 45FN, in a 1:1 molar stoichiometry, for 1 h at room temperature. After dilution in Laemmli sample buffer (without SDS or reducing agents), the complexes or individual proteins were loaded on a 4-15% TGX gradient gel (Biorad). Electrophoresis was performed at 125 V for 75 min, using ice-cold running buffer and with the gel chamber submerged in an ice bath.

Microplate protein-binding assay

Coating of microtiter plates was performed in TBS, whereas all other incubation steps were performed in TBS containing 0.1% Tween-20. Microtiter plates were coated overnight at 4°C with human plasma FN (10 μg/ml) or 45FN (5 μg/ml). To compare binding of WT and truncated TG2 to FN, Sf9-produced TG2 or TG2 1-465 (1.5 μg/ml) were added in a three-fold dilution series, and plates were incubated for 1 h at 37°C. TG2 was detected with biotinylated 693-1-E01 anti-TG2 mAb (0.5 μg/ml) followed by alkaline phosphatase-conjugated streptavidin (Southern Biotech). After addition of phosphatase substrate, absorbance was measured at 405 nm in a microplate reader (Thermo Scientific). To assess the effect of TG2 conformation in the binding to FN, effector-free, GDP-bound or inhibitor/calcium-bound TG2 (1.5 μg/ml, prepared as described above) was added to the

plates and three-fold serially diluted in effector-containing buffer. After 1 h incubation at 37°C, TG2 was detected with 0.5 µg/ml mouse anti-TG2 mAb CUB7402 (Thermo Scientific) followed by alkaline phosphatase-conjugated goat anti-mouse IgG (Abcam) and detection as described above. To assess the effect of TG2 mutations on the binding of TG2-reactive mAbs targeting different TG2 epitopes, plates were coated overnight at 4°C with WT TG2 or TG2 mutants (3µg/ml). After adding TG2-reactive mAbs three-fold serially diluted, plates were incubated for 1 h at 37°C, followed by alkaline phosphatase-conjugated rabbit anti-human IgG (Abcam) and detection as described above.

Hydrogen/deuterium exchange and mass spectrometry

Deuterium labeling of iTG2 alone or iTG2 in complex with 45FN was carried out as described previously for complexes of TG2 and anti-TG2 mAbs (Iversen et al. 2014). Briefly, isotopic exchange was initiated by a 10-fold dilution of iTG2 solution (11 µM iTG2, 50 mM Tris-HCl, 150 mM NaCl, 5 mM CaCl2, pH 7.4) in the presence or absence of an equimolar concentration of 45FN into deuterated buffer (pH 7.7, uncorrected value for the isotope effect at the glass electrode) with the same composition as the nondeuterated buffer. Deuteration was carried out at 25°C for 10, 100, 1000 and 10000 seconds. The backbone amide isotopic exchange reaction was quenched by formic acid acidification (pH 2.5) followed by freezing in liquid N2. Mass spectrometric analyses of the deuterium labeled samples were carried out with an electrospray ionization Time-of-Flight mass spectrometer coupled to a cooled reversed-phased UPLC with on-line pepsin digestion (Waters HDX manager) as described previously (Iversen et al. 2014).

SPR binding assay

45FN was immobilized on CM5 sensor chips (~ 200 resonance units) through amine-coupling chemistry, according to the instructions from the manufacturer. SPR was carried out at 25°C with a Biacore 3000 instrument (GE Healthcare). The coupling was performed with the amine coupling kit (GE Healthcare) by injecting 2.5 µg/mL of 45FN diluted into 10 mM sodium acetate (pH 4.5) (GE Healthcare); unreacted groups were blocked by injection of 1 M ethanolamine-HCl. Hepes-buffered saline-EP (0.01 M Hepes, pH7.4, 0.15 M NaCl, 3mM EDTA, 0.005% surfactant P20) was used as running buffer and dilution buffer. Injections of TG2 variants were performed at a flow rate of 70 µl/min; the injection time was 1 min, and the dissociation time was 10 min. Regeneration of the sensor chips was performed with a single injection of NaOH (10 mM) for 150 s at a flow rate of 50 µL/min. All SPR experiments

were conducted with effector-free TG2 proteins, with the exception of experiments involving truncated TG2 1-465 which was used as inhibitor-bound enzyme. For assessing the relative binding to 45FN, 100 nM of each TG2 variant was injected. Binding kinetic constants were determined by injecting serial dilutions of TG2 WT and the mutant variants. Binding data were zero-adjusted, and the reference cell values were subtracted. The Langmuir 1:1 ligand binding model or the steady-state affinity binding model provided by the BIAevaluation software (version 4.1) were used to determine the binding kinetics.

RESULTS

Binding of TG2 to FN is independent of TG2 conformation and the C-terminal domains

Complex formation between TG2 and FN was initially monitored by non-denaturing PAGE. To determine whether binding to FN requires full-length TG2, we compared 45FN complex formation with full-length TG2 (WT) and a truncated version of TG2 having intact N-terminal and core domains but lacking the two C-terminal domains (corresponding to the first 465 amino acid residues; TG2 1-465). Proteins were preincubated in a 1:1 molar ratio before electrophoretic separation. We found that both WT TG2 and TG2 1-465 were able to form a complex with 45FN with comparable efficiency, as no band corresponding to free 45FN could be observed (Fig. 1a). Thus, TG2 binding to FN does not require the presence of the C-terminal domains of TG2. In agreement with this observation, WT TG2 and TG2 1-465 showed comparable binding to full-length FN or 45FN using microplate protein-binding assay (Fig. 1b).

We next addressed whether TG2 conformation influences the ability to bind FN. The two conformational states of TG2 can be separated and visualized by non-denaturing PAGE due to the considerable difference in the hydrodynamic radius between open and closed conformations. GDP-bound TG2 (closed conformation) (Liu et al. 2002; Jang et al. 2014) and inhibitor-bound TG2 (iTG2; open conformation) (Pinkas et al. 2007) were equally able to generate a complex with 45FN (Fig. 1c). Also in microplate protein-binding assay we found no influence of TG2 conformation on the ability to bind 45FN or full-length FN (Fig. 1d). In summary, binding to FN is independent of TG2 conformation and the C-terminal domains of TG2. Importantly, the structure of the N-terminal domain of TG2 is unaffected by the conformational state of TG2 (Liu et al. 2002; Pinkas et al. 2007; Iversen et al. 2014).

Analysis of the FN-binding site of TG2 by HDX-MS

In order to map the interaction site of FN on TG2, we analyzed TG2 and TG2 bound to FN by hydrogen/deuterium exchange coupled with mass spectrometry (HDX-MS). Backbone amide hydrogens are replaced with deuterons upon protein incubation in D_2O, and the level of deuterium incorporation in any region of the protein will depend on exposure to the solvent and whether the backbone is involved in hydrogen bonding. Hydrogen atoms concealed within a folded protein or involved in binding will display significantly slower exchange rates than hydrogen atoms in flexible regions at the protein surface. Regions of a protein that are

involved in a binding event will typically display reduced deuterium uptake due to the formation of stable hydrogen bonds and direct shielding from the solvent upon binding. Thus, by using MS to assess the degree of deuteration in proteolytic peptides obtained from protein complexes, it is possible to map interaction interfaces. However, it should be noted that regions that are remote from the binding site may also exhibit a reduced deuterium uptake upon complexation through allosteric effects. Additional binding assays probing the effect of the side chain on the binding affinity are therefore required to ascertain that a reduced deuterium uptake is caused by protection against exchange in the binding interface.

We compared the incorporation of deuterium at the peptide level (local-exchange analysis) in iTG2 alone or iTG2 in a complex with 45FN. Regions with reduced deuterium uptake upon FN binding (highlighted in yellow in Fig. 2a) are located mainly in the N-terminal domain of TG2. Peptide fragments comprising amino acids 41-58, 120-129 and 130-135 showed most pronounced decrease in deuterium exchange, indicating that these regions are involved in FN binding whereas only slight reduction in deuterium uptake was observed for peptide fragments 5-12 and 59-81. Additionally, several overlapping peptide fragments in the core domain showed reduced exchange (amino acids 195-219), suggesting that residues within this domain could participate in the interaction with FN. No change in the incorporation of deuterium was detected in peptides from the C-terminal domains of TG2 (Fig. 2a and Supplemental Fig. 1), supporting our observation that FN binding is independent of these domains. Interestingly, no change in the deuterium uptake was observed in peptide fragment 89-100 (Supplemental Fig. 1), which contains amino acid residues D94 and D97 previously established as critical residues for FN binding (Hang et al. 2005).

TG2 residues involved in binding to FN

Based on the HDX/MS results and previous data indicating an overlap between the FN-binding site and a common epitope targeted by anti-TG2 antibodies in celiac disease (epitope 1) (Cardoso et al. 2015), we wished to address the importance of selected amino acid residues in the binding to FN. In order to do so, we generated TG2 mutants and evaluated their binding to 45FN by SPR. We first exchanged the entire N-terminal domain of TG2 with the N-terminal domain of TG3 (TG3/TG2 chimeric protein). As expected, this completely abolished binding to FN (Fig. 3a). Importantly, a truncated TG2 variant consisting of only the N-terminal domain (the first 143 amino acid residues; TG2 1-143) was still capable of binding to 45FN, although with apparently lower affinity than full-length TG2. These data show that the

N-terminal domain of TG2 is both necessary and sufficient to maintain binding, although parts of the core domain could also contribute to the interaction (Fig. 3a). We next generated and tested TG2 variants carrying single-amino acid substitutions for binding to FN. As previously observed, the mutants K30E, R116A and H134A of TG2 showed impaired binding to immobilized 45FN as analyzed by SPR (Fig. 3b) (Cardoso et al. 2015). We next examined how combinations of these mutations would influence FN binding by injecting equal amounts of the TG2 R116A/H134A (RH) and K30E/R116A/H134A (KRH) mutants. Indeed, the 45FN binding responses of the double and triple mutants were dramatically reduced as compared to WT TG2 (Fig. 3b). Thus, we identified three amino acid residues within the N-terminal domain of TG2 that serve as key players in the high affinity interaction with FN.

Based on our HDX-MS data and analysis of the three-dimensional structure of TG2, we wished to address whether also other residues of TG2 would be critical for binding to FN, as the binding interface of FN likely spans a larger area than the three residues identified so far. To address involvement of TG2 regions identified by HDX-MS (41-58, 120-135, 195-219) in binding to FN, we mutated selected residues and compared their binding to FN using SPR. In addition, we analyzed mutant K265S for binding to FN, as K265 was previously shown to be important for recognition by anti-TG2 celiac mAb (Chen et al. 2015). No effect was seen for E51Q, D187A, D191A and K265S mutants (Fig. 3c). However, a slight reduction in binding was observed T58A, E120A, S129A and D198A (data not shown). We therefore determined the binding kinetics of the mutants that showed the most pronounced impaired binding to 45FN (Fig. 3d and Table 1). For this purpose, we injected serial dilutions (50.0-1.5 nM) of each of the TG2 variants over immobilized 45FN and fitted the obtained sensorgrams to a simple Langmuir 1:1 binding model. In addition, as the mutants R116A/H134A (RH) and K30E/R116A/H134A (KRH) displayed severely reduced binding (Fig. 3b), increased protein concentrations (10.0-0.7 µM or 15.0-0.1 µM, respectively) were injected in order to allow fitting to a steady state affinity binding model (Fig. 3d). The selected TG2 mutants showed distinct binding kinetics compared to WT TG2 or truncated variant (TG2 1-465), which gave very similar kinetic parameters (Table 1). Specifically, the S129A mutant showed only slightly reduced binding (2-fold) that was solely due to faster dissociation while E120A reduced binding to 45FN by more than 12-fold as a result of both altered association and dissociation rates. Further, the mutations T58A and D198A reduced binding to 45FN by 37- and 86-fold, respectively, due to slower association rates (Table 1). For the mutants R116A/H134A (RH) and K30E/R116A/H134A (KRH) the derived binding kinetics revealed

both greatly altered association and dissociation rates that translated into 400- and more than 2000-fold reduced binding to 45FN, respectively (Table 1). In addition, steady-state affinity measurements at near-equilibrium binding responses for the RH and KRH mutants confirmed their weak binding affinities (Table 1). In summary, we demonstrate the involvement of residues from both the N-terminal and core domains of TG2 in the interaction with FN.

As depicted in Fig. 4a, the residues that have the strongest effect on FN binding, K30, R116 and H134, are located in close proximity in the three-dimensional structure of TG2. Interestingly, these residues are either party or fully evolutionarily conserved in TG2 (Fig. 4b) but not present in other transglutaminase family members (Fig. 4c), in agreement with their inability to bind FN. Residues R116 and H134 are highly conserved whereas K30 is in six out of fifteen species, with a conservative arginine substitution in the remaining nine species (Fig. 4b).

Mutations that affect binding to FN also interfere with the binding of epitope 1-targeting anti-TG2 mAbs

We previously found that some residues involved in binding to FN are part of the epitope recognized by epitope 1 celiac disease anti-TG2 mAbs (Cardoso et al. 2015; Chen et al. 2015). To address the degree of overlap between epitope 1 and the FN-binding site, we tested whether our identified TG2 mutants displaying reduced FN binding were still recognized by epitope 1 mAbs. In agreement with previous observations, epitope 1 mAb 679-14-E06 did not recognize the TG2 mutants R116A/H134A and K30E/R116A/H134A in microplate protein-binding assay (Fig. 5). In addition, this mAb did not recognize D198A, suggesting that also this particular residue is part of epitope 1. None of the other TG2 mutants showed reduced binding by epitope 1 mAb, and none of the mutations influenced significantly the recognition of TG2 by epitope 2 (763-4-B06) or epitope 3 mAbs (693-1-E01) (Fig. 5). These antibodies recognize conformational epitopes on TG2, thus verifying the correct folding of our TG2 mutants. However, removal of the entire N-terminal domain of TG2, as in the chimeric TG3/TG2 protein, abrogated recognition of epitope 1 as well as epitope 2 and epitope 3 mAbs.

DISCUSSION

In this study we have identified residues required for high-affinity binding of TG2 to FN. We show that the binding to FN is independent of conformational state and does not require presence of the C-terminal domains of TG2. In agreement with previous reports we found binding to be mediated by the N-terminal domain (Jeong et al. 1995; Hang et al. 2005). Binding involved residues K30, T58, R116, E120, S129 and H134, where mutation of residues K30, R116 and H134 dramatically reduced binding to FN. We further showed that the interaction extends to the catalytic core domain, as mutation of residue D198 reduces binding affinity. The residues K30, R116 and H134 are partly or fully evolutionarily conserved among species, but not present in other transglutaminase family members, underscoring the importance of this interaction in TG2 biology and function.

FN is abundantly expressed in the ECM and is an important structural constituent that mediates cell migration, signaling and survival (Akimov et al. 2000; Akimov and Belkin 2001; Verderio et al. 2003). The interaction between TG2 and the 45 kDa gelatin-binding domain of FN is very specific and of unusually high affinity. In fact, biotinylated 45FN specifically recognizes TG2 in tissue sections, and no binding is observed by 45FN in TG2 KO tissue (Cardoso et al. 2015). Here, we identify highly conserved positively charged residues of TG2 that act as key players in binding to 45FN. Binding of TG2 does not depend on glycosylation or other post-translational modification, as FN fragments in phage-display can also bind TG2 (Di Niro et al. 2010). Thus, this interaction likely relies on negatively charged residues in the 45FN domain.

Validity of experiments that address binding of TG2 mutant proteins to FN relies on the stability and correct folding of the expressed proteins. In this study we only included proteins that were produced in good yield and which could be purified by affinity chromatography to high purity with no presence of aggregates. Most importantly, all mutants were recognized by anti-TG2 mAbs that bind non-linear epitopes and are sensitive to changes in TG2 conformation, verifying correct folding (Iversen et al. 2013). Thus, the effects we observe on FN or epitope 1 mAb binding by introduction of mutations in TG2, likely reflect the targeting of residues in the binding interface.

TG2 has been shown to play a role in cell-matrix interactions and to mediate cell adhesion and migration by acting as an integrin-binding co-receptor for FN (Akimov et al. 2000; Akimov and Belkin 2001). Increased TG2 expression has been reported in many types of cancers, particularly metastatic tumors (Yakubov et al. 2013; Eckert et al. 2015; He et al. 2015). In ovarian cancer, this has been linked to increased cell adhesion on FN, promoting cancer cell migration and survival (Satpathy et al. 2007; Cao et al. 2008; Cao et al. 2012). To understand and be able to specifically modulate the binding between TG2 and FN may thus be of value for certain types of malignancies (Yakubov et al. 2014). TG2 has also been shown to interact with the heparan sulfate chains of syndecan-4 (Scarpellini et al. 2009) and indeed TG2 residues 262–265 have been shown to form a cluster involved in the binding to heparin (Lortat-Jacob et al. 2012). Although FN has high affinity to both TG2 and heparin/syndecan-4, TG2 binding to syndecan-4 is independent of FN (Scarpellini et al. 2009). As the FN- and heparin-binding site of TG2 are located separately and we found residue K265 not to be involved in the binding to FN, it is conceivable that the three proteins could form a ternary complex mediated by TG2.

In the extracellular space, TG2 presumably adopts an open conformation due to high Ca^{2+} concentrations. We found that binding to FN is not influenced by the conformational state of TG2. In agreement with this observation, we found that the FN-binding site is located apart from where the two C-terminal beta-barrel domains fold over the catalytic core domain in the closed, GTP-bound conformation. Thus, TG2 should retain sufficient flexibility to allow for movement of the two C-terminal domains, and also to allow for enzymatic activity, when bound to FN. Previous studies indicate that TG2 is indeed active upon binding to FN, but that activity is reduced compared to unbound TG2 (Verderio et al. 2003). Whether this relies on conformational changes induced in TG2 upon binding to FN, or steric hindrance, remains unknown.

In celiac disease, patients develop autoantibodies that target extracellular TG2. Curiously, the dominant epitope, epitope 1, overlaps with the FN binding site (Cardoso et al. 2015). We here identify additional overlap between FN and epitope 1 through D198, thus extending into the catalytic core domain. It is not yet known whether this overlap is coincidental or of biological significance, but it is possible that the shielding of epitope 1 through binding of TG2 to FN promotes escape from negative selection of epitope 1-targeting B cells in the bone marrow, thereby allowing them to differentiate into autoantibody-producing plasma cells in celiac

disease. Given the high affinity of the interaction between TG2 and FN, it is unlikely that TG2 can be displaced once bound to FN. We have however recently demonstrated that TG2 has an additional interaction partner in the ECM, as epitope 1 antibodies do recognize ECM-bound TG2 (Cardoso et al. 2015). The details and biological significance of this novel interaction are still not clear, but it is possibly this fraction of extracellular TG2 that is available for peripheral B-cell recognition and uptake in celiac disease.

Although TG2 has other interaction partner(s) in the ECM, the interaction with FN is considered fundamental to most biological functions ascribed to extracellular TG2. Better understanding of this interaction requires knowledge of the binding interface, which we here have mapped. Future work should aim at determining whether binding to FN also induces allosteric changes that may influence enzymatic activity.

Conflict of Interest: The authors declare that they have no conflict of interest.

This article does not contain any studies with human participants or animals performed by any of the authors.

References

Achyuthan KE, Rowland TC, Birckbichler PJ, et al (1996) Hierarchies in the binding of human factor XIII, factor XIIIa, and endothelial cell transglutaminase to human plasma fibrinogen, fibrin, and fibronectin. Mol Cell Biochem 162:43–9.

Adamczyk M, Griffiths R, Dewitt S, et al (2015) P2X7 receptor activation regulates rapid unconventional export of transglutaminase-2. J Cell Sci Sci 128:4615–28.

Akimov SS, Belkin AM (2001) Cell surface tissue transglutaminase is involved in adhesion and migration of monocytic cells on fibronectin. Blood 98:1567–76.

Akimov SS, Krylov D, Fleischman LF, Belkin AM (2000) Tissue transglutaminase is an integrin-binding adhesion coreceptor for fibronectin. J Cell Biol 148:825–38.

Bergamini CM, Signorini M, Poltronieri L (1987) Inhibition of erythrocyte transglutaminase by GTP. Biochim Biophys Acta 916:149–51.

Cao L, Petrusca DN, Satpathy M, et al (2008) Tissue transglutaminase protects epithelial ovarian cancer cells from cisplatin-induced apoptosis by promoting cell survival signaling. Carcinogenesis 29:1893–1900.

Cao L, Shao M, Schilder J, et al (2012) Tissue transglutaminase links TGF-β, epithelial to mesenchymal transition and a stem cell phenotype in ovarian cancer. Oncogene 31:2521–2534.

Cardoso I, Stamnaes J, Andersen JT, et al (2015) Transglutaminase 2 interactions with extracellular matrix proteins as probed with celiac disease autoantibodies. FEBS J 282:2063–75.

Chen X, Hnida K, Graewert MA, et al (2015) Structural basis for antigen recognition by transglutaminase 2-specific autoantibodies in celiac disease. J Biol Chem 290:21365–21375.

Clarke DD, Mycek MJ, Neidle A, Waelsch H (1959) The incorporation of amines into protein. Arch Biochem Biophys 79:338–54.

Di Niro R, Sulic A-M, Mignone F, et al (2010) Rapid interactome profiling by massive sequencing. Nucleic Acids Res 38:e110.

Eckert RL, Fisher ML, Grun D, et al (2015) Transglutaminase Is a Tumor Cell and Cancer Stem Cell Survival Factor. Mol Carcinog 54:947–58.

Engvall E, Ruoslahti E, Miller EJ (1978) Affinity of fibronectin to collagens of different genetic types and to fibrinogen. J Exp Med 147:1584–95.

Erat MC, Slatter DA, Lowe ED, et al (2009) Identification and structural analysis of type I

collagen sites in complex with fibronectin fragments. Proc Natl Acad Sci U S A 106:4195–200.

Foss S, Watkinson RE, Grevys A, et al (2016) TRIM21 Immune Signaling Is More Sensitive to Antibody Affinity Than Its Neutralization Activity. J Immunol 196:3452–59.

Fuller GM, Doolittle RF (1966) The formation of crosslinked fibrins: evidence for the involvement of lysine epsilon-amino groups. Biochem Biophys Res Commun 25:694–700.

Furie M, Rifkin D (1980) Proteolytically derived fragments of human plasma fibronectin and their localization within the intact molecule. J Biol Chem 255:3134–40.

Hang J, Zemskov EA, Lorand L, Belkin AM (2005) Identification of a novel recognition sequence for fibronectin within the NH2-terminal β-sandwich domain of tissue transglutaminase. J Biol Chem 280:23675–83.

He W, Sun Z, Liu Z (2015) Silencing of TGM2 reverses epithelial to mesenchymal transition and modulates the chemosensitivity of breast cancer to docetaxel. Exp Ther Med 10:1413–1418.

Iversen R, Di Niro R, Stamnaes J, et al (2013) Transglutaminase 2-specific autoantibodies in celiac disease target clustered, N-terminal epitopes not displayed on the surface of cells. J Immunol 190:5981–91. doi: 10.4049/jimmunol.1300183

Iversen R, Mysling S, Hnida K, et al (2014) Activity-regulating structural changes and autoantibody epitopes in transglutaminase 2 assessed by hydrogen/deuterium exchange. Proc Natl Acad Sci U S A 111:17146–51.

Jang TH, Lee DS, Choi K, et al (2014) Crystal structure of transglutaminase 2 with GTP complex and amino acid sequence evidence of evolution of GTP binding site. PLoS One 9:1–8.

Jeong JM, Murthy S, Radek JT, Lorand L (1995) The fibronectin-binding domain of transglutaminase. J Biol Chem 270:5654–8.

LeMosy EK, Erickson HP, Beyer WF, et al (1992) Visualization of purified fibronectin-transglutaminase complexes. J Biol Chem 267:7880–5.

Liu S, Cerione R a, Clardy J (2002) Structural basis for the guanine nucleotide-binding activity of tissue transglutaminase and its regulation of transamidation activity. Proc Natl Acad Sci U S A 99:2743–2747.

Lorand L, Graham RM (2003) Transglutaminases: crosslinking enzymes with pleiotropic functions. Nat Rev Mol Cell Biol 4:140–56.

Lortat-Jacob H, Burhan I, Scarpellini A, et al (2012) Transglutaminase-2 interaction with

heparin: identification of a heparin binding site that regulates cell adhesion to fibronectin-transglutaminase-2 matrix. J Biol Chem 287:18005–17.

Molberg O, Mcadam SN, Körner R, et al (1998) Tissue transglutaminase selectively modifies gliadin peptides that are recognized by gut-derived T cells in celiac disease. Nat Med 4:713–7.

Mosesson MW, Chen AB, Huseby RM (1975) The cold-insoluble globulin of human plasma: Studies of its essential structural features. Biochim Biophys Acta 386:509–524.

Mycek MJ, Clarke DD, Neidle A, Waelsch H (1959) Amine Incorporation into Insulin as Catalyzed by Transglutaminase. Arch Biochem Biophys 84:528–40.

Pankov R (2002) Fibronectin at a glance. J Cell Sci 115:3861–3863.

Piacentini M, D'Eletto M, Farrace MG, et al (2014) Characterization of distinct sub-cellular location of transglutaminase type II: changes in intracellular distribution in physiological and pathological states. Cell Tissue Res 358:793–805.

Pinkas DM, Strop P, Brunger AT, Khosla C (2007) Transglutaminase 2 undergoes a large conformational change upon activation. PLoS Biol 5:e327.

Radek JT, Jeong JM, Murth S, et al (1993) Affinity of human erythrocyte transglutaminase for a 42-kDa gelatin-binding fragment of human plasma fibronectin. Proc Natl Acad Sci U S A 90:3152–6.

Ruoslahti E, Hayman EG, Engvall E, et al (1981) Alignment of biologically active domains in the fibronectin molecule. J Biol Chem 256:7277–7281.

Satpathy M, Cao L, Pincheira R, et al (2007) Enhanced peritoneal ovarian tumor dissemination by tissue transglutaminase. Cancer Res 67:7194–7202.

Scarpellini A, Germack R, Lortat-Jacob H, et al (2009) Heparan sulfate proteoglycans are receptors for the cell-surface trafficking and biological activity of transglutaminase-2. J Biol Chem 284:18411–23.

Sollid LM, Molberg O, McAdam S, Lundin KEA (1997) Autoantibodies in coeliac disease: tissue transglutaminase--guilt by association? Gut 41:851–2.

Stamnaes J, Fleckenstein B, Sollid LM (2008) The propensity for deamidation and transamidation of peptides by transglutaminase 2 is dependent on substrate affinity and reaction conditions. Biochim Biophys Acta - Proteins Proteomics 1784:1804–1811.

Stamnaes J, Pinkas DM, Fleckenstein B, et al (2010) Redox regulation of transglutaminase 2 activity. J Biol Chem 285:25402–9.

Stephens P, Grenard P, Aeschlimann P, et al (2004) Crosslinking and G-protein functions of transglutaminase 2 contribute differentially to fibroblast wound healing responses. J Cell

Sci 117:3389–403.

Telci D, Wang Z, Li X, et al (2008) Fibronectin-tissue transglutaminase matrix rescues RGD-impaired cell adhesion through syndecan-4 and β1 integrin co-signaling. J Biol Chem 283:20937–47.

Turner P, Lorand L (1989) Complexation of fibronectin with tissue transglutaminase. Biochemistry 28:628–35.

Verderio EAM, Telci D, Okoye A, et al (2003) A novel RGD-independent cel adhesion pathway mediated by fibronectin-bound tissue transglutaminase rescues cells from anoikis. J Biol Chem 278:42604–14.

Yakubov B, Chelladurai B, Schmitt J, et al (2013) Extracellular Tissue Transglutaminase Activates Noncanonical NF-κB Signaling and Promotes Metastasis in Ovarian Cancer. Neoplasia 15:609–19.

Yakubov B, Chen L, Belkin AM, et al (2014) Small molecule inhibitors target the tissue transglutaminase and fibronectin interaction. PLoS One 9:e89285.

Zemskov EA, Janiak A, Hang J, et al (2006) The role of tissue transglutaminase in cell-matrix interactions. Front Biosci 11:1057–76.

Zemskov EA, Mikhailenko I, Hsia R-C, et al (2011) Unconventional secretion of tissue transglutaminase involves phospholipid-dependent delivery into recycling endosomes. PLoS One 6:e19414.

Figure legends

Fig. 1 Binding between FN and different conformational states of TG2. Complex formation between TG2 and 45FN assessed by non-denaturing PAGE (**a**, **c**) or microplate protein-binding assay with detection of bound TG2 using anti-TG2 human mAb 693-1-E01 (**b**) or mouse mAb CUB7402 (**d**). Either full-length (WT) or truncated (1-465) TG2 was used (**a**, **b**). To address the effect of conformation, WT TG2 was incubated with GDP (closed conformation), with peptide inhibitor and $CaCl_2$ (iTG2, open conformation), or left untreated in the effector-free state (**c**, **d**). Protein complexes between TG2 and 45FN are marked with an asterisk (*)

Fig. 2 HDX-MS analysis of the complex between iTG2 and 45FN. (**a**) TG2 peptides with reduced D-uptake in the presence of 45FN are highlighted in yellow in the TG2 structure (PDB 2Q3Z). The structure was designed using PyMOL software. (**b**) Deuterium uptake plots for TG2 peptides which showed reduced deuterium uptake in the 45FN-bound state (red curves) compared to the unbound state (blue curves). Error bars represent SD based on labeling triplicates

Fig. 3 SPR sensorgrams showing binding of different TG2 variants to immobilized 45FN. The binding responses are given as resonance units (RU) and were recorded as a function of time (seconds). (**a**-**c**) Injection of equal amounts (100 nM) of different TG2 variants over immobilized 45FN. (**a**) Effect of replacement or deletion of individual TG2 domains. The binding response obtained with the N-terminal domain of TG2 alone (TG2 1-143) is markedly lower than that of WT TG2 due to its smaller molecular weight. (**b**) Effect of mutating residues K30, H134 and R116 alone or in combination. (**c**) Single amino acid TG2 mutants that did not affect the binding to 45FN and for which kinetic parameters were not derived. (**d**) Determination of the binding kinetics for different TG2 variants by injection of serial concentrations over immobilized 45FN

Fig. 4 Evolutionary conservation of positively charged TG2 residues involved in FN binding. (**a**) Location of the FN-binding site in the three-dimensional structure of the N-terminal and (partial) catalytic domains of TG2 (PDB 4PYG). The residues K30, R116 and H134 (in red) are essential for binding to FN. Residues T58, E120, S129 and D198 (in orange) are conceivably involved in the interaction with FN. The figure was designed using PyMOL software. (**b**) ClustalW amino acid sequence alignment of the N-terminal sequence of TG2 derived from 15 species. The amino acid residues 30, 116 and 134 that were subjected to site-direct mutagenesis in human TG2 are highlighted in yellow; in bold, conserved residues among species; in red, conservative mutations. (**c**) ClustalW amino acid sequence alignment of human transglutaminases (TG1-TG7) and mouse TG2

Fig. 5 The effect of TG2 mutations on the binding of TG2-reactive mAbs targeting different TG2 epitopes assessed by a microplate protein binding assay. Binding of epitope 1 mAb (circles) was affected by mutations D198A, R116A/H134A and K30E/R116A/H134A (KRH). Binding of epitope 2 (squares) or epitope 3 (triangles) mAbs to TG2 mutants was not affected (T58A, E120A, S129A, D187A), or affected to a lesser extent (D198A, KRH)

Supplementary Figures

Supplementary Fig. 1 Deuterium uptake plots for all identified TG2 peptides which showed no difference in D-uptake when comparing the 45FN-bound state (red curves) and the unbound state (blue curves). Error bars represent SD based on labeling triplicates

Figure 1

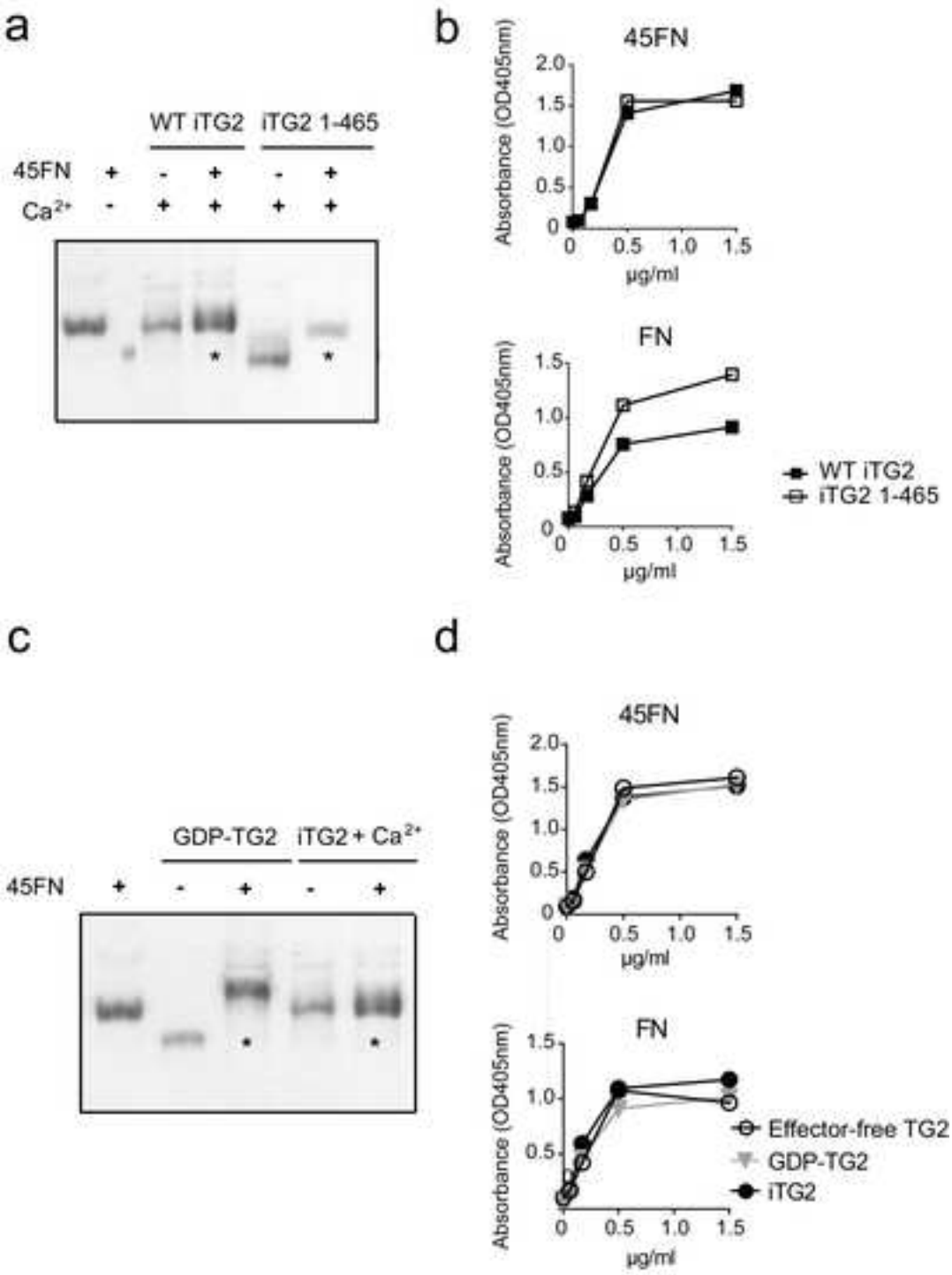

Figure 2

a

b

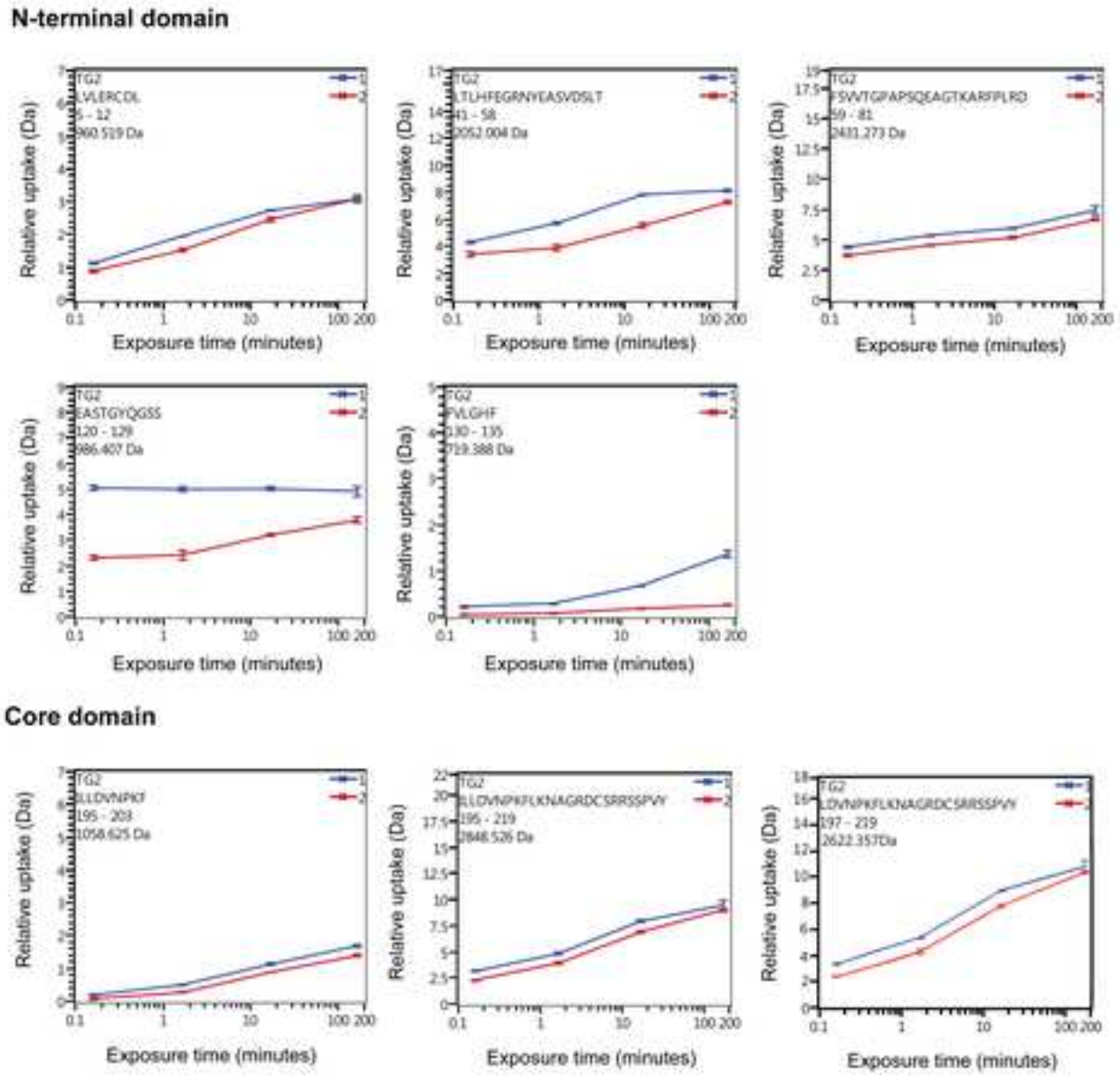

Figure 3

Click here to download Figure Fig.3_edited.tif

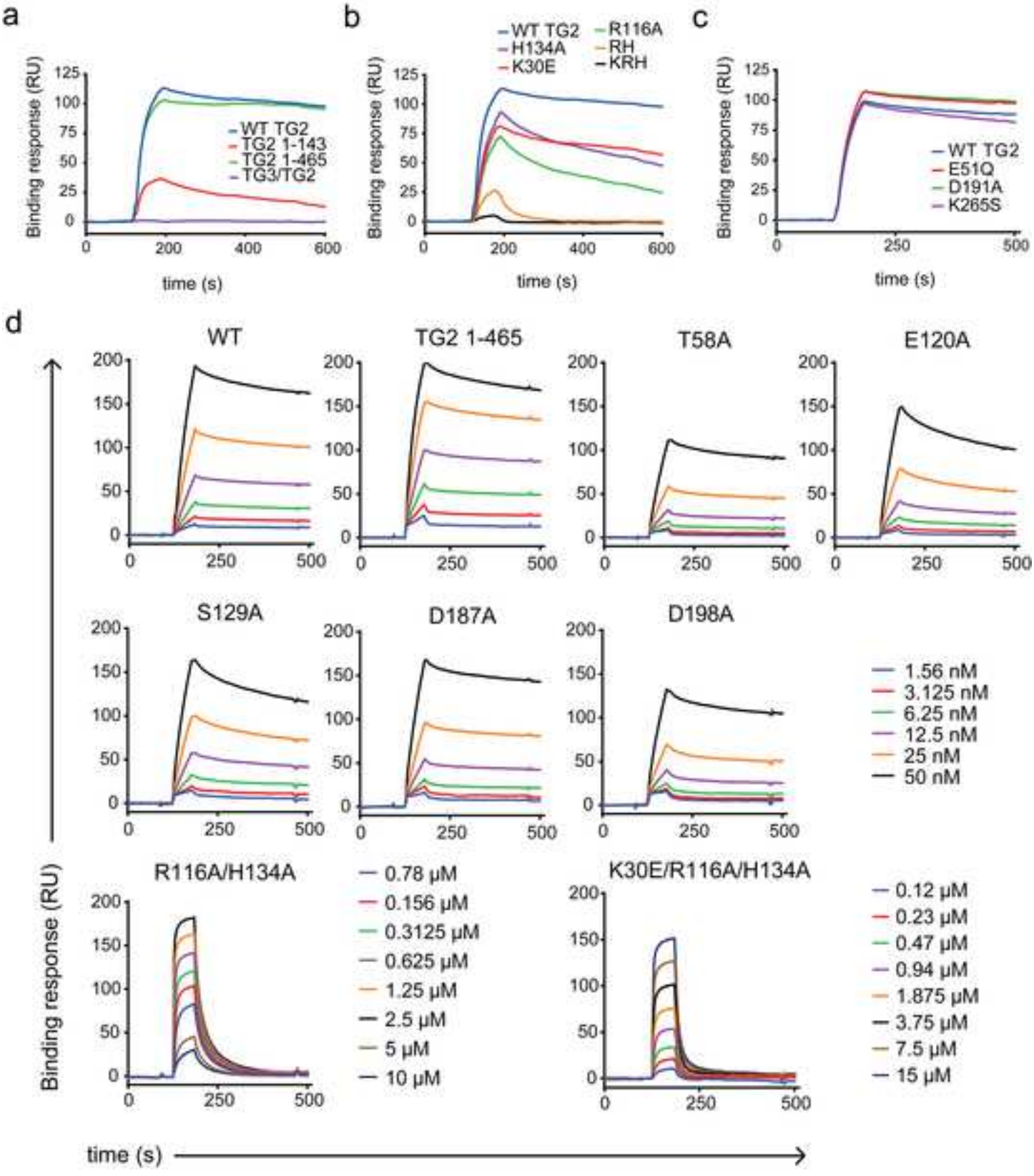

Figure 4

Click here to download Figure fig.4_edited.tif

a

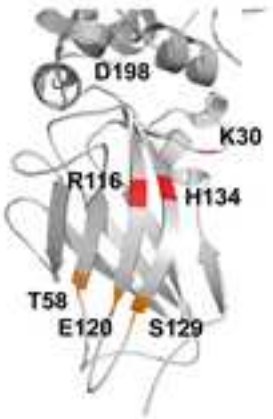

b

```
                          30                  116                 134
Human          HTADLCREKLVVRRG--APIGLYRLSLEAS--SFVLGHFILLF
Orangutan      HTADLCREKLVVRRG--APIGLYRLSLEAS--SFVLGHFILLF
Macaque        HTADLCREKLVVRRG--APIGLYRLSLEAS--SFVLGHFILLF
Cat            HTADLCREKLVVRRG--APIGLYRLSLEAS--SFVLGHFILLF
Rat            HTADLCQQKLVLRRG--APVGQYRLSLETS--SFMLGHFILLF
Mouse          HTADLCQEKLVLRRG--APIGLYRLSLEAS--SFVLGHFILLY

Horse          YTADLCRERLVVRRG--APIGLYRLSLEAS--SFVLGHFTLLF
Elephant       HTANLCQERLVVRRG--APIGLYRLSLETS--SFVLGHFILLF
Pig            HTADLCRERLVVRRG--APIGLYRLNLEAS--SFLLGHFTLLF
Dog            HTAGLCQGRLVVRRG--APVGLYRLSLEAS--SFVLGHFTLLF
Guinea pig     RTADLCREHLVLRRG--APIGLYRLSLEAS--SFVLGHFILLY
Rabbit         HTADLCQDRLVVRRG--APIGLYRLSLEAS--SFVLGHFTLLF
Giant Panda    HTADLCRDRLVVRRG--APIGLYRLSLEAS--SFVLGHFTLLF

Sheep          HTADLCRERLVVRRG--APIGHYRLSLEAS--SFMLAQFTLLF
Cow            HTADLCREHLVVRRG--GTKALFRLSDATE--SFMLGQFTLLF
```

c

```
                          30                  116                 134
hTG2           HTADLCREKLVVRRG--APIGLYRLSLEAS--SFVLGHFILLF
mTG2           HTADLCQEKLVVRRG--APIGLYRLSLEAS--SFVLGHFILLY
TG1            HTDEYEYDELIVRRG--AIIGKFQFTVRTQ--FDPRNEIYILF
TG3            HTDKFSSQELILRRG--APIGRYTMALQIF--SVKLGTFILLF
TG4            HTWEFQTSSPVFRRG--AILGKYQLNVKTG--KSEENILYLLF
TG5            HTEEITVDHLLVRRG--AAVGRYLLKIHID--AYQLGEFILLF
TG6            HTQEYPCPELVVRRG--AVIGRYLLSIRLS--NRRLGEFVLLF
TG7            HTQEMGVKRLTVRRG--AVIGHYTLKIEIS--TYPLGTFILLF
```

Figure 5

Click here to download Figure Fig.5_edited.tif

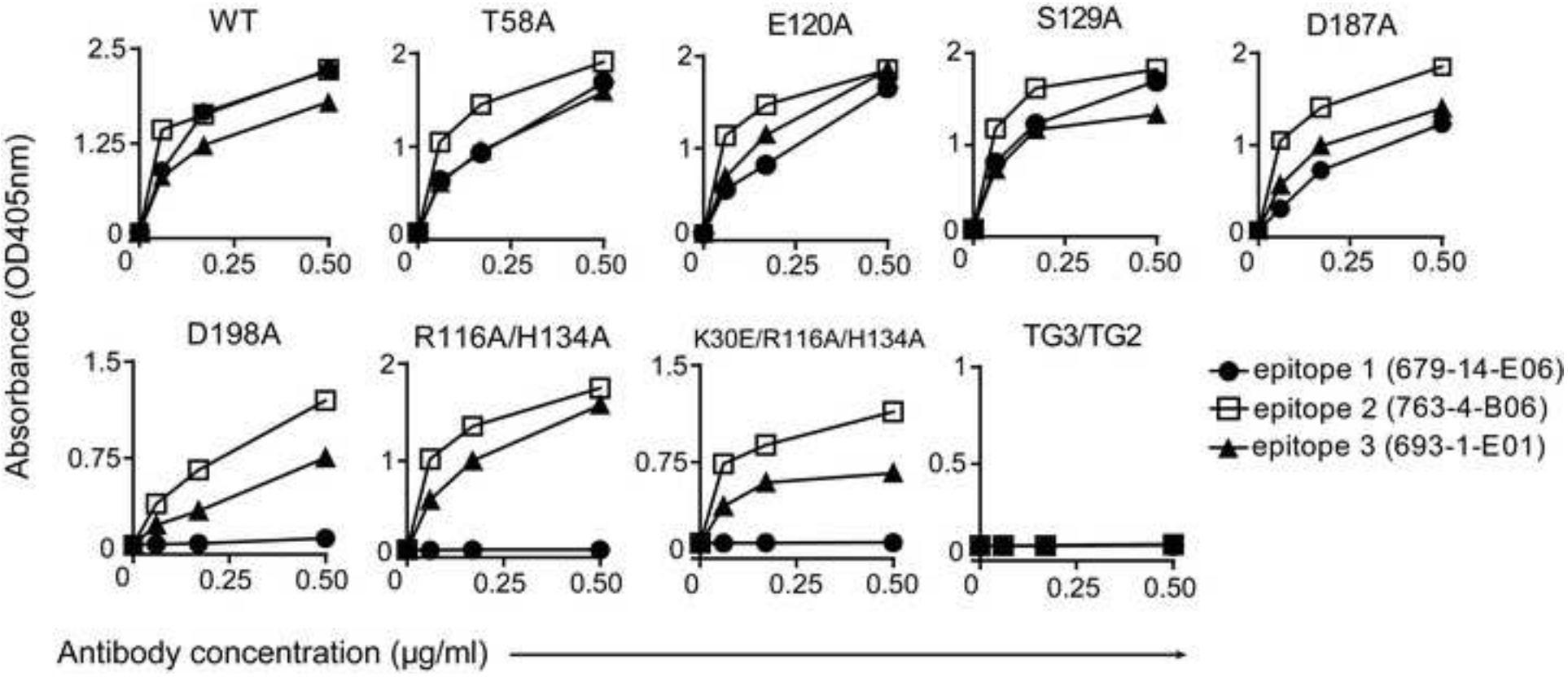

Table

Table 1: SPR-derived binding kinetics for the interaction between different TG2 variants and immobilized 45FN. The kinetic rate constants were obtained by fitting the data to a simple first-order (1:1) Langmuir bimolecular interaction model or by using a steady state affinity binding model where indicated. The kinetic values represent the average of duplicates. The standard deviation is indicated.

TG2 variant	ka ($10^5/M^{-1}s^{-1}$)	kd ($x10^{-4}/s^{-1}$)	KD (*nM*)	Steady- state KD (*nM*)
WT	3.3 ± 0.3	3.1 ± 0.1	0.9 ± 0.1	ND
TG2 1-465	9.2 ± 0.4	3.6 ± 0.5	0.3 ± 0.0	ND
T58A	0.1 ± 0.0	3.8 ± 0.3	33.6 ± 1.3	ND
E120A	0.7 ± 0.1	8.5 ± 0.2	11.5 ± 0.6	ND
S129A	3.6 ± 0.2	6.6 ± 0.5	1.9 ± 0.2	ND
D187A	1.9 ± 0.1	2.5 ± 0.2	1.3 ± 0.1	ND
D198A	0.05 ± 0.01	3.7 ± 0.3	78.2 ± 2.3	ND
R116A/H134A	ND	ND	ND	451.0
K30E/R116A/H134A	ND	ND	ND	2170.0

ND – Not determined